Role for ADAP in shear flow–induced platelet mechanotransduction

Ana Kasirer-Friede,[1] Zaverio M. Ruggeri,[2] and Sanford J. Shattil[1]

[1]Department of Medicine, University of California San Diego, La Jolla; and [2]Department of Molecular and Experimental Medicine, The Scripps Research Institute, La Jolla, CA

Binding of platelets to fibrinogen via integrin αIIbβ3 stimulates cytoskeletal reorganization and spreading. These responses depend on tyrosine phosphorylation of multiple proteins by Src family members and Syk. Among Src substrates in platelets is adhesion- and degranulation-promoting adapter protein (ADAP), an adapter with potential binding partners: SLP-76, VASP, and SKAP-HOM. During studies of platelet function under shear flow, we discovered that ADAP$^{-/-}$ mouse platelets, unlike ADAP$^{+/+}$ platelets, formed unstable thrombi in response to carotid artery injury. Moreover, fibrinogen-adherent ADAP$^{-/-}$ platelets in shear flow ex vivo showed reduced spreading and smaller zones of contact with the matrix. These abnormalities were not observed under static conditions, and they could not be rescued by stimulating platelets with a PAR4 receptor agonist or by direct αIIbβ3 activation with $MnCl_2$, consistent with a defect in outside-in αIIbβ3 signaling. ADAP$^{+/+}$ platelets subjected to shear flow assembled F-actin–rich structures that colocalized with SLP-76 and the Rac1 exchange factor, phospho-Vav1. In contrast, platelets deficient in ADAP, but not those deficient in VASP or SKAP-HOM, failed to form these structures. These results establish that ADAP is an essential component of αIIbβ3-mediated platelet mechanotransduction that promotes F-actin assembly and enables platelet spreading and thrombus stabilization under fluid shear stress. (Blood. 2010;115: 2274-2282)

Introduction

During hemostasis, platelets must mount a strong and rapid response under a variety of hydrodynamic shear stresses.[1] Bidirectional signaling involving integrin αIIbβ3 is particularly important for hemostasis.[1,2] Once platelets contact the damaged vessel wall, the ligand binding function of αIIbβ3 is activated by "inside-out" signals that stabilize adhesion and initiate platelet aggregation. In turn the binding of multivalent adhesive ligands, such as fibrinogen, to αIIbβ3 triggers "outside-in" signals that promote platelet cytoskeletal rearrangements, spreading, and optimal thrombus formation. Although the conversion of force into biochemical signals (mechanotransduction) in response to hydrodynamic shear stresses has been extensively studied in endothelial cells and demonstrated to elicit activation of ion channels, extracellular signal-regulated kinases, and rho GTPases,[3] there is still debate as to whether and how force transmission occurs via adhesion receptors and cytoskeletal elements in other adherent cells, including platelets.[4,5] A few careful studies of platelets have pointed to shear-dependent roles for proteins, such as phosphoinositide 3-kinase,[6] $P2Y_1$,[7] and α-actinin[8] at high arterial or pathologic shear. Overall, however, mechanotransduction in platelets, and the role of αIIbβ3 in this process in particular, remain poorly understood.

Adhesion- and degranulation-promoting adapter protein (ADAP) is a hematopoietic-specific protein that promotes cytokine production, proliferation, and integrin-mediated adhesion after stimulation of T lymphocytes through the T-cell receptor.[9,10] In these cells, ADAP forms a signaling module by binding to the SH3 domain of SKAP-55[11] and can bind this domain within the SKAP-55 homologue, SKAP-HOM, as well.[12] Of note, SKAP-55 interacts with RIAM, a Rap1 effector, to promote increases in integrin affinity.[13] ADAP also possesses binding sites for the interaction domains of several other proteins, among them the SH2 domains of SLP-76 and Fyn, the EVH1 domain of VASP, and the MAGUK region of CARMA1,[10,14] and ADAP can bind phosphoinositols through 2 helically extended SH3 domains.[15] In mouse platelets, genetic deletion of ADAP reduces but does not eliminate inside-out activation of αIIbβ3 in response to von Willebrand factor (VWF) binding to GP Ib-IX-V or ADP/thrombin binding to G protein–coupled receptors.[16] ADAP localizes to the periphery of human platelets spread on fibrinogen.[17] In the present study, we provide evidence that ADAP is a critical component of αIIbβ3-mediated outside-in signaling by virtue of its regulation of the platelet actin cytoskeleton in the face of hemodynamic shear stresses.

Methods

Reagents and antibodies

Rhodamine phalloidin was from Molecular Probes/Invitrogen. Rabbit polyclonal antibodies against Vav1 pTyr-174 were from Abcam and Santa Cruz Biotechnology. Rabbit polyclonal antibodies against VASP, c-Src pTyr-418, and SLP-76 were from Alexis Biochemicals, Biosource/Invitrogen, and Cell Signaling Technology, respectively. Mouse monoclonal antibody against vinculin was from Sigma-Aldrich. Rat monoclonal antibody against GP IX was from Emfret Analytics. A polyclonal sheep antibody against murine ADAP was a kind gift from Gary Koretzky (University of Pennsylvania). Dimeric, murine A1A2 VWF (dmA1A2

Submitted August 12, 2009; accepted November 6, 2009. Prepublished online as *Blood* First Edition paper, December 7, 2009; DOI: 10.1182/blood-2009-08-238238.

An Inside *Blood* analysis of this article appears at the front of this issue.

The online version of this article contains a data supplement.

The publication costs of this article were defrayed in part by page charge payment. Therefore, and solely to indicate this fact, this article is hereby marked "advertisement" in accordance with 18 USC section 1734.

VWF) was prepared as described.[16] SuperSignal WestPico reagent was from Pierce Chemicals. All other reagents were from Sigma-Aldrich.

Mouse strains

Mice deficient in ADAP, SKAP-HOM, or VASP have been described[18-21] and were obtained from Gary Koretzky, Ben Neel, (Ontario Cancer Institute), and Alexander Clowes (University of Washington), respectively. $ADAP^{+/+}$, $SKAP\text{-}HOM^{+/+}$, and $VASP^{+/+}$ mice represent littermate controls. All mouse studies were conducted with Institutional Animal Care and Use Committee approval from the University of California, San Diego, including in vivo thrombosis studies and ex vivo studies with mouse blood.

Carotid artery injury model

Thrombus formation in the mouse carotid artery was induced with 3.75% anhydrous ferric chloride ($FeCl_3$) as described.[22] The carotid artery was subsequently excised, fixed in 4% formaldehyde for 4 hours at 4°C, transferred to 70% ethanol, and paraffin embedded, and sections were mounted on slides and stained with hematoxylin and eosin. Histology was examined by the use of a Leica DMLS microscope fitted with a Leica Plan 20×/0.4 numeric aperture (NA) objective, and SPOT software (Diagnostic Instruments).

Flow studies

Mouse blood preparation is described in the supplemental Methods (available on the *Blood* website; see the Supplemental Materials link at the top of the online article). Whole blood was diluted 1:1 with Walsh buffer to permit quantitative studies of platelets on the matrix surface, and 10 μg/mL mepacrine was added to label platelets for adhesion studies. Glass coverslips were coated overnight at 4°C, with either 50 μg/mL fibrinogen or 10 μg/mL dmA1A2 VWF domain fragment, matrices that are engaged primarily by adhesion receptors αIIbβ3 and GPIb-IX-V, respectively. After rinsing with HEPES buffer (20mM HEPES [*N*-2-hydroxyethylpiperazine-*N*′-2-ethanesulfonic acid], 150mM NaCl, pH 7.4), coverslips were exposed to flowing blood in a parallel plate flow chamber as described.[23] Images were acquired at 2 separate preset positions, recorded with a Sony SVO-9500MD camera at 30 fps, and data were stored on a Terabyte server. The evolution of close cell-surface contact area in platelets captured from flow was monitored by reflection interference contrast microscopy (RICM).[24-26] Major advantages of this technique are that no exogenous reagents are required for cell detection, object visualization is limited to a maximum range of 30 to 100 nm from the cell-surface interface, and distance is depicted as a quantifiable gradient of gray intensities.[27] Images were recorded in real time at a minimum of 3 preset positions during 5 time cycles by use of a Sony DXC 390 CCD camera (Sony Corp).

To show that major differences exist in the dynamics of adhesion and spreading as a direct consequence of exposure to shear stress and to exclude differences in methodology as the basis for the defects in ADAP spreading under flow, we investigated platelet surface interactions by RICM in real time by using identical blood preparations and experimental setup under both static and flow conditions (supplemental Figure 1). To test the effect of soluble agonist stimulation on platelet spreading, a platelet monolayer was generated during the course of 1.5 minutes at 500 s^{-1}, and then platelets were perfused with buffer containing 0.25mM PAR4 receptor-activating peptide, 0.5mM $MnCl_2$, or vehicle. When inhibitors were used, they were added to blood 15 minutes before perfusion through the device.

After monitoring live platelet attachment and spreading kinetics, surface-interacting platelets were fixed with 3.7% formaldehyde[28,29] without cessation of flow (perfusion fixation) to maintain hydrodynamic fluid shear stress during fixation. Although this step was sufficient to immediately freeze motion and preserve morphological characteristics, incubation with formaldehyde was continued for another 5 minutes. Then coverslips were carefully removed from the flow chamber, rinsed, permeabilized, blocked with 10% goat serum, and stained with antibodies against proteins of interest and appropriate secondary antibodies and/or fluorescently labeled phalloidin to stain F-actin.[28] Western blots[30] were performed to confirm that all antibodies used detected a single protein band of expected molecular weight in platelet lysates. Images of postflow, fixed, and stained platelets were captured with a Deltavision deconvolution microscope (Applied Precision Inc) and Nikon 100×/1.4 NA oil objective with the use of a Photometrics Sony Coolsnap HQ camera and Softworks acquisition software (Applied Precision Inc) at the University of California, San Diego Cancer Center Core Microscopy Facility. Identical acquisition settings were used for all slides derived under equivalent experimental conditions. Deconvolved images were saved as TIF files and analyzed for protein phosphorylation and localization.

Image analyses

Further details of image analyses are described in the supplemental Methods.

Platelet assays under static conditions

To investigate adhesion under static conditions, we tested the ability of $ADAP^{+/+}$ and $ADAP^{-/-}$ platelets to adhere at a range of input fibrinogen coating concentrations. Adhesion was quantified with an alkaline phosphatase assay.[31] Nonspecific binding was determined by subtracting residual fluorescence in bovine serum albumin-coated wells. To examine platelet spreading under static conditions, washed $ADAP^{+/+}$ and $ADAP^{-/-}$ platelets resuspended at 2×10^7/mL in Walsh buffer were added to 18-mm coverslips coated with 100 μg/mL fibrinogen and incubated for 1 hour at 37°C in the presence or absence of PAR4 receptor-activation peptide or $MnCl_2$. Alternatively, blood suspensions prepared for flow studies were applied to fibrinogen-coated coverslips in the flow chamber without perfusion, and spreading under static conditions was monitored by RICM. Adherent platelets were stained with rhodamine-phalloidin for F-actin, and images were acquired as described previously.

Statistical analyses

Analysis of variance was performed by the use of the Student *t* test for unpaired samples.

Results

$ADAP^{-/-}$ mice do not form a stable thrombus after arterial injury

Hemostasis appears compromised in $ADAP^{-/-}$ mice, as evidenced by rebleeding upon tail-vein transection.[16] Therefore, we assessed the capacity of $ADAP^{-/-}$ mice to form occlusive thrombi after carotid artery injury by $FeCl_3$, a thrombosis model dependent on platelets as well as fibrin deposition. The average blood flow before $FeCl_3$ injury was similar in $ADAP^{+/+}$ and $ADAP^{-/-}$ mice (1.1 ± .05 mL/min). At 5% to 7% $FeCl_3$ concentration, thrombus formation was comparable for $ADAP^{-/-}$ and $ADAP^{+/+}$ littermates. To test whether less severe vessel injury would uncover a role for ADAP in thrombus formation, we decreased the $FeCl_3$ concentration to 3.75%, which reproducibly induced vessel occlusion in wild-type mice. In $ADAP^{-/-}$ mice, however, vessel occlusion was significantly decreased at this concentration.

As illustrated in Figure 1A, carotid artery blood flow tracings from all $ADAP^{+/+}$ mice demonstrated reduced blood flow and complete occlusion within an average of 10 minutes after application of 3.75% $FeCl_3$. In contrast, $ADAP^{-/-}$ mice typically exhibited cyclic flow changes indicative of dispersion and/or embolization of growing thrombi over time, a pattern previously observed with defects in outside-in αIIbβ3 signaling.[32-34] The average time to first occlusion was prolonged in $ADAP^{-/-}$ mice ($P < .01$; Figure 1B), and 30 minutes after the lesion, 78% of $ADAP^{-/-}$ but 0% of

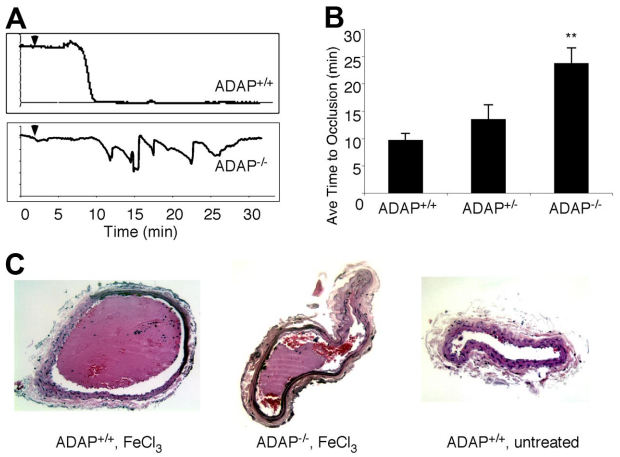

Figure 1. ADAP$^{-/-}$ mice exhibit abnormal thrombus formation in vivo. (A) Representative carotid artery blood flow tracings from ADAP$^{+/+}$ and ADAP$^{-/-}$ mice. A filter paper impregnated with 3.75% $FeCl_3$ was applied for 3 minutes (▼), and blood flow was monitored for an additional 25 minutes. (B) The average time to first occlusion was determined for each mouse, and results are shown as the average ± SEM of at least 7 mice per strain. *$P < .01$. (C) Hematoxylin and eosin–stained sections through the carotid artery excised 30 minutes after application of $FeCl_3$ (ADAP$^{+/+}$, left; ADAP$^{-/-}$, middle) or buffer (ADAP$^{+/+}$, right).

ADAP$^{+/+}$ mice exhibited patent arteries (n = 8; $P < .01$). Histologic examination of carotid arteries excised 30 minutes after $FeCl_3$ injury confirmed the presence of large, occlusive thrombi in ADAP$^{+/+}$ arteries as opposed to smaller, nonocclusive thrombi in ADAP$^{-/-}$ arteries (Figure 1C left and middle). Arteries of ADAP$^{+/+}$ mice treated with isotonic saline instead of $FeCl_3$ were free of thrombus (Figure 1C right). Thus, under these experimental conditions, the absence of ADAP reduces the capacity of mice to develop a stable, occlusive carotid artery thrombus after a less severe vessel injury.

Stable attachment to fibrinogen and outside-in αIIbβ3 signaling are compromised in ADAP$^{-/-}$ platelets under shear flow

Given the particular hemostatic phenotype observed in ADAP$^{-/-}$ mice, we examined the function of ADAP$^{-/-}$ platelets in whole blood under conditions of shear stress, focusing on the known αIIbβ3 contribution to stable platelet attachment and spreading under these conditions.[23,35] Indeed, stable attachment of ADAP$^{-/-}$ platelets to fibrinogen-coated coverslips was compromised under shear flow. Under the conditions used, an average of 900 and 800 ADAP$^{+/+}$ and ADAP$^{-/-}$ platelets, respectively, contacted the surface in equivalent image fields examined over a 70-second period. ADAP$^{-/-}$ platelets consistently showed a decrease in the percent of total surface contacting platelets able to sustain attachment to fibrinogen for between 2 and 30 seconds, relative to ADAP$^{+/+}$ platelets. Approximately 30% fewer platelets remained attached for 2 to 4 seconds, and longer-term adhesion was increasingly ADAP dependent, because approximately 40% to 50% fewer platelets remained attached for 6 seconds or up to 30 seconds (n = 4; $P < .05$, $P < .01$; paired Student t test; Figure 2A). As controls, no stable platelet adhesion was observed during an equivalent time period when ADAP$^{+/+}$ blood was perfused over coverslips coated with bovine serum albumin or over fibrinogen in the presence of EDTA (ethylenediaminetetraacetic acid), which blocks αIIbβ3 interaction with fibrinogen. In sharp contrast to these results, ADAP$^{-/-}$ platelets adhered and spread onto fibrinogen normally under static conditions, whether platelets were unstimulated, activated by a PAR4 agonist to induce inside-out signaling, or treated with $MnCl_2$ to directly activate αIIbβ3 (Figure 2B-C; supplemental Figure 1C). Thus, ADAP is required for stable, αIIbβ3-dependent adhesion of platelets to fibrinogen under conditions of shear flow.

To evaluate the nature of the adhesion defect in more detail, platelet spreading was examined at shear rates (γ) between 50 s^{-1} and 600 s^{-1}, corresponding to the range of venous and low arterial shear rates. Platelets were perfusion fixed and stained with an antibody to GP IX to identify the plasma membrane. At all γ, even at relatively early time points (30-45 seconds), it was possible to distinguish between ADAP$^{-/-}$ and ADAP$^{+/+}$ platelets; more detailed analyses were conducted at $\gamma = 500$ s^{-1}. As shown in Figure 3A, platelets from the 2 mouse strains differed in morphology and surface area: ADAP$^{+/+}$ platelets lost the symmetrical, spherical appearance of unactivated cells; formed lamellipodia; and developed cusps from which filopodia extended (arrowhead, Figure 3A top). In contrast, ADAP$^{-/-}$ adherent platelets largely retained a spherical morphology with extended filopodia, but few lamellipodia and exhibited a significant decrease in mean surface area when perfusion-fixed (6.66 ± 1.3 μm^2), as compared with ADAP$^{+/+}$ platelets (8.93 ± 0.4 μm^2; n = 5; $P < .05$; Figure 3B).

To examine the contact areas of unfixed platelets with fibrinogen in real time under shear flow and to avoid possible fixation artifacts, we used RICM. This technique reveals objects that are at a distance of 100 nm or less from a surface and with a progression from black to white on a gray scale as the distance increases. Early ADAP$^{+/+}$ platelet attachment points (dark areas) were small (area < 1 μm^2) and central, soon followed by close adhesion contacts at filopodial tips. Central dark regions, corresponding to close contact areas, grew rapidly in ADAP$^{+/+}$ platelets as bonding surfaces

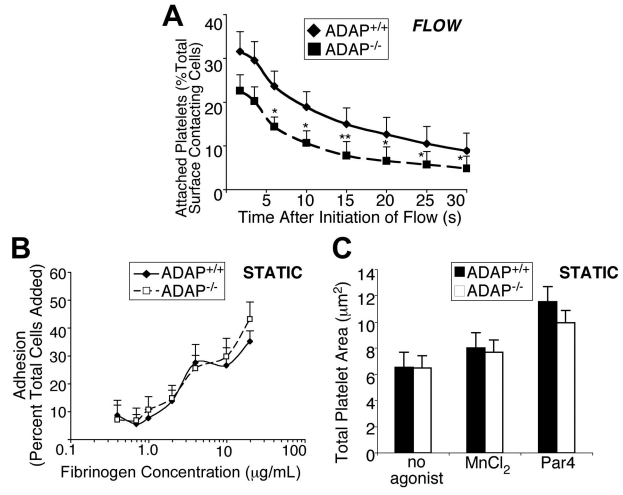

Figure 2. ADAP$^{-/-}$ platelets exhibit unstable adhesion in the presence of shear stress. (A) In vitro adhesion of platelets labeled with 10 μg/mL mepacrine to visualize platelets, under shear flow. Quantification of unfixed ADAP$^{+/+}$ or ADAP$^{-/-}$ platelets captured onto fibrinogen at $\gamma = 500$ s^{-1}. Movie clips were prepared to cover the period 10 to 80 seconds after flow initiation, and images were processed at 6 fps. The first frame was subtracted to remove already attached platelets. All platelets perfused over fibrinogen under shear flow, which appeared on the surface within the first 30 seconds, were individually tracked, and platelets remaining surface-bound for a period of 2 to 30 seconds are depicted as a percent of total surface-contacting cells. Results presented are the average of 4 separate experiments ± SEM (*$P < .05$; **$P < .01$, paired Student t test). (B) Platelet adhesion to fibrinogen under static conditions. Washed platelets were plated for 60 minutes in wells coated with increasing concentrations of fibrinogen, and adhesion was determined by an alkaline phosphatase assay. Results show the percent of total platelets added that remained adherent, and are an average of at least 3 separate experiments ± SEM. (C) Mean surface areas of platelets spread onto fibrinogen under static conditions. Washed platelets were plated onto fibrinogen with or without 250μM PAR4-activating peptide or 0.5mM $MnCl_2$, allowed to spread for 60 minutes at 37°C, then fixed, permeabilized and stained for F-actin with the use of rhodamine phalloidin. Results presented are the average of 3 separate experiments ± SEM.

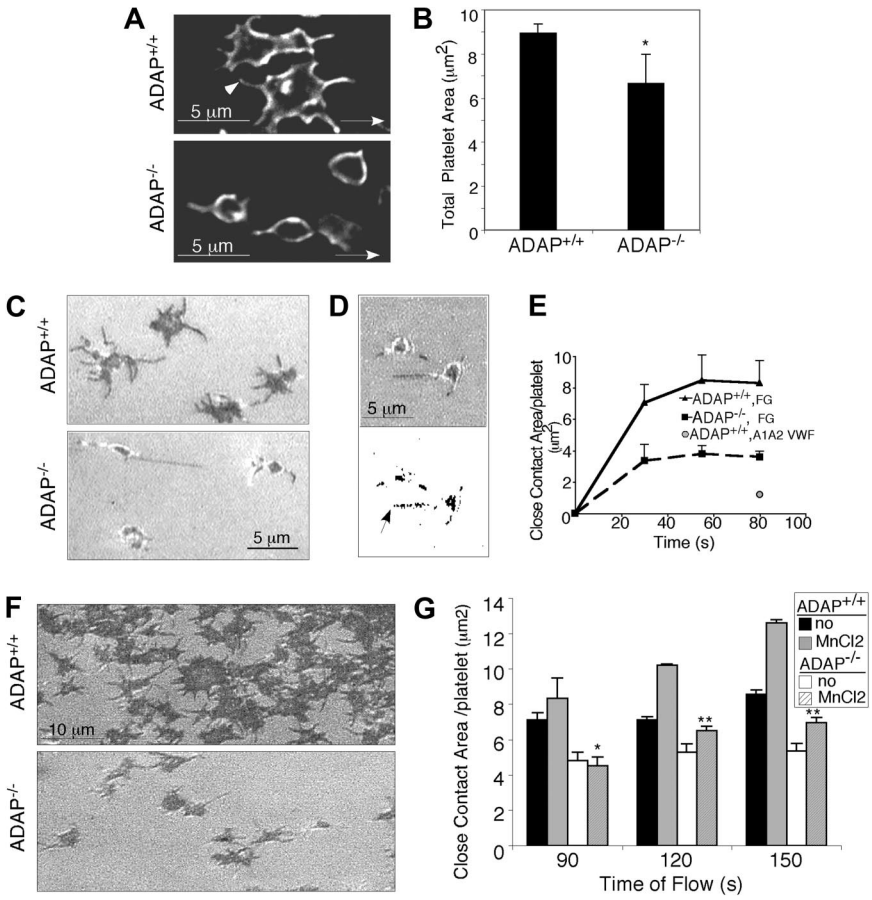

Figure 3. ADAP$^{-/-}$ platelets have an outside-in spreading defect under shear flow. (A) Deconvolved microscopic images of adherent ADAP$^{+/+}$ (top) and ADAP$^{-/-}$ (bottom) platelets fixed without cessation of flow, permeabilized, and stained with an antibody against the membrane receptor, GP IX (acquired at 100× magnification). (B) Areas of perfusion-fixed platelets were quantified by the use of Image Pro Plus software. Results are the average of 5 separate experiments ± SEM (*$P < .05$). (C-G). Images of unfixed spreading platelets under shear flow conditions were acquired in real time by RICM. (C) Close platelet/surface contacts (dark regions) in platelets captured onto fibrinogen after 1.5 minutes of flow (acquired at 60× magnification). (D) Close platelet/surface contact areas in an image acquired 20 seconds after initiation of flow: shown as the original unthresholded image (top) or after thresholding and binarization (bottom) for quantification. (E) Average close surface contact area per platelet as a function of time upon interaction with immobilized fibrinogen (F-G) or a dmA1A2 VWF fragment (quantified with Image Pro Plus). Results are representative of at least 3 separate experiments ± SEM. (F) RICM images of close platelet-surface contact areas in unfixed platelets captured onto fibrinogen and stimulated with a PAR4 agonist for 1 minute under shear flow. (G) Quantification of close surface contact areas in platelets captured onto fibrinogen and directly stimulated with the extrinsic integrin activator, $MnCl_2$ for 1 minute under shear flow. Results are the average of 3 separate experiments ± SEM (*$P < .05$; **$P < .01$).

extended during spreading (Figure 3C top) but remained smaller in ADAP$^{-/-}$ platelets (Figure 3C bottom; supplemental Video 1) at all time points tested. Quantification of the average close contact area/platelet over time (an example of a thresholded and binarized image used for this measurement is shown in Figure 3D), confirmed the smaller size ($P < .05$) in ADAP$^{-/-}$ platelets as compared with ADAP$^{+/+}$ platelets (Figure 3E). The surface contact area of ADAP$^{-/-}$ platelets on fibrinogen was similar to that seen on a dmA1A2 VWF domain fragment (Figure 3E) that lacks binding sites for αIIbβ3 and supports only transient interactions. Continued monitoring by RICM indicated that establishment of close contact formation in ADAP$^{-/-}$ platelets remained reduced even after 3 minutes from flow initiation. Moreover, the defective ability of ADAP$^{-/-}$ platelets to form close contacts with and spread on fibrinogen could not be rescued by stimulation of platelets with a PAR4 agonist or with $MnCl_2$ (Figure 3F-G). Taken together, these results indicate that ADAP is required for the normal growth of platelet contact areas and spreading on fibrinogen under shear flow conditions. Furthermore, because $MnCl_2$ bypasses any need for inside-out signaling to activate αIIbβ3, the results are consistent with a defect in outside-in αIIbβ3 signaling in ADAP$^{-/-}$ platelets.

ADAP$^{-/-}$ platelets exhibit impaired cytoskeletal reorganization under shear flow

Because of the structural role of the actin cytoskeleton and its potential contribution to platelet anchorage under flow conditions, we sought first to establish the normal F-actin distribution in ADAP$^{+/+}$ platelets captured onto fibrinogen within 45 seconds, 1.5 minutes, or 3 minutes of shear flow. From the earliest time point analyzed, we observed the formation of small actin-rich structures (Figure 4A) that increased in number and size over time. Concurrently, platelets increased their total surface areas, and the actin structures persisted and accumulated during the course of 3 minutes, with surprisingly few platelets producing the actin stress cables characteristic of platelets spread under static conditions.[36] We hypothesized that if ADAP were to play a role in actin polymerization and spreading, then it would potentially be found associated with actin or with actin-regulatory molecules. Indeed, we found that ADAP colocalized with actin in these structures in ADAP$^{+/+}$ platelets (Figure 4A top; Figure 4B). However, in ADAP$^{-/-}$ platelets captured from flow, actin-rich structures were greatly reduced and usually asymmetrically distributed (Figure 4A bottom), even after 3 minutes. Vinculin, a hallmark of focal complexes and adhesions, localized to the actin-rich structures in ADAP$^{+/+}$ platelets but was not clustered in ADAP$^{-/-}$ platelets (not shown). To quantify the frequency and size of these structures in platelet images, we calculated an arbitrary "cluster index" equal to (average cluster area) × (average cluster number/platelet). Single-cell analysis of the actin cluster index for a minimum of 150 ADAP$^{+/+}$ and ADAP$^{-/-}$ platelets confirmed the decreased assembly of actin-rich structures in ADAP$^{-/-}$ platelets adherent to fibrinogen (Figure 4C), which had a cluster index similar to that for ADAP$^{+/+}$ platelets unstably interacting with a dmA1A2 VWF fragment. The vinculin cluster index was also significantly lower in ADAP$^{-/-}$ platelets (0.32 ± 0.02) than in ADAP$^{+/+}$ platelets (0.84 ± 0.07; $n = 3$; $P < .01$). In contrast, under static conditions,

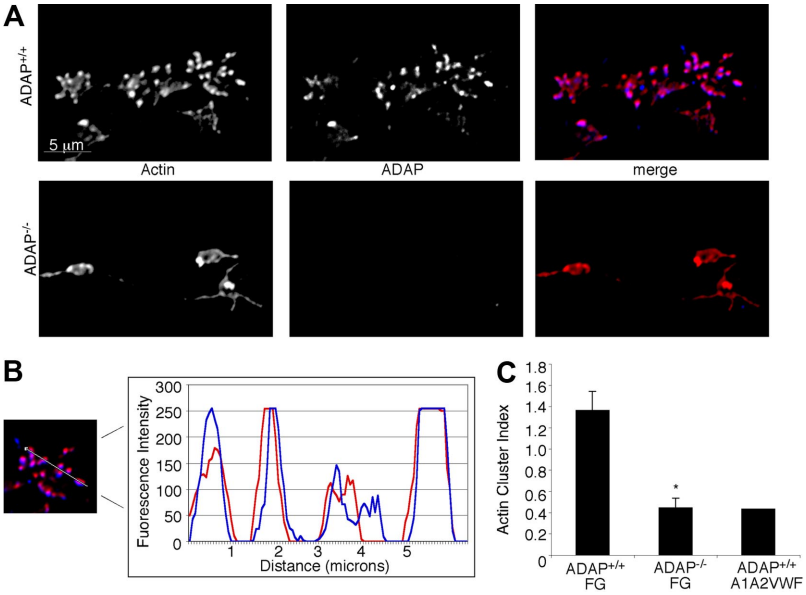

Figure 4. Intracellular actin distribution in platelets adhering to fibrinogen under flow. Platelets adherent to fibrinogen were perfusion-fixed after 1.5 minutes of flow, permeabilized and stained for F-actin (red) and ADAP (blue). (A) Actin-rich structures form in ADAP$^{+/+}$ platelets adherent to fibrinogen, in which ADAP is also found (top). These structures were greatly reduced in ADAP$^{-/-}$ platelets (bottom), in which ADAP staining was negative. (B) Line profile of actin and ADAP fluorescence distribution in a representative ADAP$^{+/+}$ platelet; note the almost identical localization. (C) Quantification of actin-rich structures in platelets perfused either over immobilized fibrinogen or a dmA1A2 VWF fragment, the latter lacking binding sites for αIIbβ3. A cluster index, used to express quantitatively the distribution of actin-rich structures, was calculated as follows: (average cluster area) × (average number of clusters per platelet). The results shown are the means ± SEM of 3 separate experiments on fibrinogen (*$P < .01$) and 2 experiments on dmA1A2 VWF fragment.

actin-rich structure formation was normal in ADAP$^{-/-}$ platelets adherent to fibrinogen (not shown). Thus, under shear flow conditions, ADAP is required for αIIbβ3-dependent actin organization into structures that also contain vinculin.

Dysregulation of ADAP binding partners and downstream effectors in ADAP$^{-/-}$ platelets under flow

Platelet adhesion to fibrinogen via αIIbβ3 initiates a signaling cascade (Figure 5A) that includes activation of Src and Syk protein tyrosine kinases and ADAP phosphorylation. Mice deficient in the ADAP binding partner, Fyn, have normal adhesion under flow and spreading on full-length VWF.[37] However, several ADAP binding partners have been implicated in the regulation of actin downstream of integrins, both in primary cells and model cell systems. For example, SLP-76 can promote lamellipodia formation when overexpressed in Chinese hamster ovary cells,[17] polarization of T cells,[38] and platelet spreading on fibrinogen[39,40]; similarly, VASP can promote actin polymerization[41] and filopodia formation[42]; and SKAP-HOM can function as a phosphoinositol-gated switch for sustaining membrane ruffles.[43] However, the functional hierarchy of these molecules relative to ADAP has not been established in platelets. Accordingly, we investigated how ADAP may interface with its binding partners in fibrinogen-adherent platelets under flow.

We found that platelet adhesion to fibrinogen under flow induced the phosphorylation of Src at Tyr-418, an event concomitant with Src activation, and this was observed even in the absence of ADAP. Staining of perfusion-fixed ADAP$^{+/+}$ and ADAP$^{-/-}$ platelets captured onto fibrinogen showed similar overall localization of Src pTyr-418 to filopodial protrusions (Figure 5B), but there was an additional localization of activated Src to actin-rich clusters in ADAP$^{+/+}$ platelets. Image quantification revealed no differences between ADAP$^{+/+}$ and ADAP$^{-/-}$ platelets in Src pTyr-418 signal (Figure 5C). In contrast, staining for SLP-76 revealed major abnormalities in ADAP$^{-/-}$ platelets. In ADAP$^{+/+}$ platelets, SLP-76 was dispersed throughout the cytoplasm and occasionally found as punctae after 45 to 90 seconds of flow, but by 3 minutes SLP-76 colocalized to actin-rich structures (Figure 6A left). However in ADAP$^{-/-}$ platelets, SLP-76 remained primarily dispersed throughout the cytoplasm with occasional punctae (Figure 6A right). Vav1

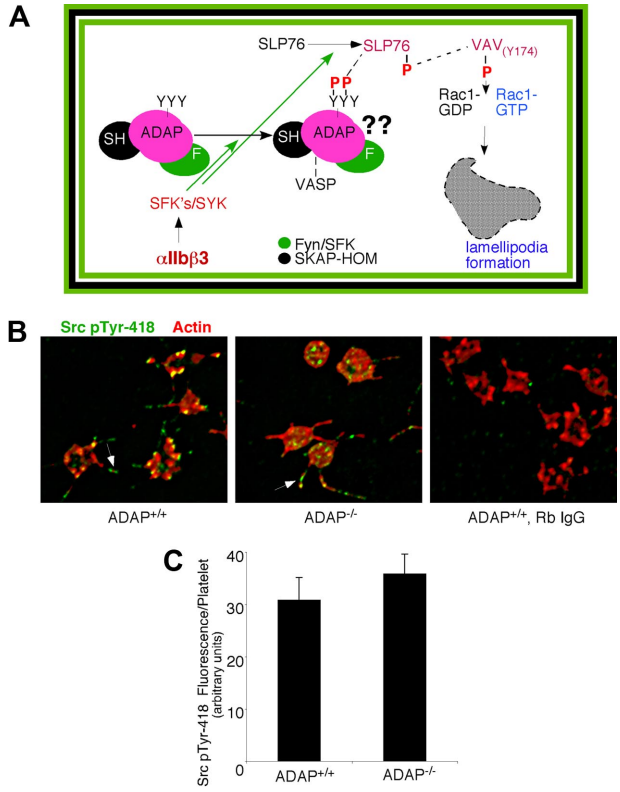

Figure 5. Early αIIbβ3-mediated outside-in signaling. (A) Schematic representation of select signaling intermediates in αIIbβ3-induced lamellipodia formation and spreading under static conditions.[2] Fibrinogen binding to αIIbβ3 induces phosphorylation of Src family kinases and Syk, which in turn phosphorylate ADAP and SLP-76 to promote their association. ADAP is shown constitutively associated with Fyn (green oval) and SKAP-HOM (black oval). Phosphorylation of SLP-76 at tyrosines 112 and 128 induces recruitment and phosphorylation of Vav1,[40,53] thereby activating its guanine nucleotide exchange function to activate Rac1 and promote lamellipodia formation. The role of ADAP in this pathway is shown as "??" in figure. (B) Immunofluorescent staining of c-Src pTyr-418 in perfusion-fixed ADAP$^{+/+}$ (left) and ADAP$^{-/-}$ platelets (middle) adhering onto fibrinogen under flow. Note regular intervals of c-Src pTyr-418 staining along filopodia (arrows). Staining with a control rabbit IgG antibody was minimal (right). (C) Quantification of average c-Src pTyr-418 fluorescence per platelet, representing an average of 3 experiments ± SEM.

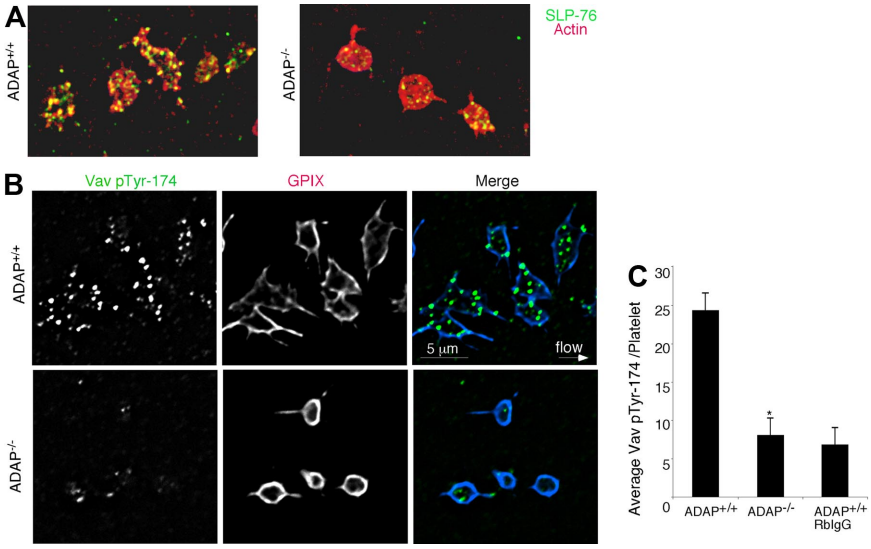

Figure 6. SLP-76 and phospho-Vav1 localization in platelets captured onto fibrinogen from shear flow. (A) ADAP$^{+/+}$ and ADAP$^{-/-}$ platelets were stained with an antibody against SLP-76 (green) and with rhodamine-phalloidin to label F-actin (red); yellow indicates colocalization. (B) Localization of Vav1 pTyr-174 in perfusion-fixed ADAP$^{+/+}$ (top) and ADAP$^{-/-}$ (bottom) platelets costained with an antibody against GP IX. Note prominent Vav1 phosphorylation in ADAP$^{+/+}$ platelets, but its almost complete absence in ADAP$^{-/-}$ platelets. Minimal nonspecific staining was seen with the use of a control rabbit IgG antibody. (C) Quantification of average Vav1 pTyr-174 fluorescence per platelet captured from flow. Results shown are the average of 3 experiments ± SEM. *$P < .05$.

is a SLP-76 binding partner that functions downstream of αIIbβ3 as an exchange factor for the actin regulator known to promote lamellipodia formation, Rac1.[17,34] Therefore, we assessed the localization of Vav1 with an antibody to Vav1 pTyr-174, a phospho-site associated with increased Vav1 exchange activity.[44] ADAP$^{+/+}$ platelets captured from flow exhibited strong phosphorylation of Vav1 Tyr-174 that was localized in large part to the actin-rich structures (Figure 6B, top). In contrast, almost no phosphorylation of Vav1 Tyr-174 was detectable in ADAP$^{-/-}$ platelets (Figure 6B, bottom), and quantification of stained images indicated a greater than 60% reduction in this phosphorylation signal (n = 3, $P < .05$; Figure 6C). Thus, ADAP is required to correctly localize a pool of SLP-76 and phospho-Vav1 in adherent platelets under flow, providing one potential explanation for the cytoskeletal and spreading defects of ADAP$^{-/-}$ platelets.

Because lamellipodial growth has been correlated with the presence of VASP at the membrane,[45] and ADAP may regulate VASP by targeting it to membrane regions, we co-stained perfusion-fixed platelets with antibodies against VASP and GP IX, the latter as a membrane marker. When 3-dimensional images were reconstructed from stacks of 0.1-μm platelet sections, VASP was found to be targeted to the membrane and to actin-rich structures in ADAP$^{+/+}$ platelets (Figure 7A). VASP targeting was significantly decreased in ADAP$^{-/-}$ platelets (% inhibition membrane targeting = 53 ± 13%, n = 3; $P < .05$; Figure 7A-B). However, when VASP$^{-/-}$ platelets were perfused over fibrinogen and compared with VASP$^{+/+}$ platelets, they showed no defects in spreading, close surface contact with the matrix, assembly of actin-rich structures, or colocalization of ADAP to these structures (Figure 7C-D). Similarly, platelets from SKAP-HOM–deficient mice functioned normally under flow (supplemental Figure 2). These results suggest that if any of the functions of VASP or SKAP-HOM are disrupted in platelets lacking ADAP, this cannot account for the phenotype of ADAP$^{-/-}$ platelets under flow.

Discussion

Studies primarily in T lymphocytes and model cell systems have implicated ADAP in outside-in signaling because ligand binding to integrins induces ADAP phosphorylation and association with actin regulatory proteins concomitant with cell motility.[9,38] However, no direct functional role for ADAP in outside-in signaling in platelets has been established. We have performed quantitative studies by using mouse models, intracellular protein staining, and live videomicroscopy of platelets in whole blood to uncover an essential role for ADAP in outside-in αIIbβ3 signaling under shear stress conditions. Our studies lead to the following conclusions: (1) ADAP is important for platelet function in vivo because ADAP-deficient mice exhibit increased frequency of rebleeding from tail bleeding wounds[16] and form unstable thrombi in the carotid artery when challenged with $FeCl_3$ (Figure 1). (2) Hydrodynamic shear stresses act as physical cues to induce αIIbβ3-dependent remodeling of the cytoskeleton in wild-type platelets (mechanotransduction) to produce platelet morphologies that minimize flow impact and maximize platelet-surface contact areas. (3) ADAP is an essential component of platelet mechanotransduction mechanisms under shear flow because ADAP$^{-/-}$ platelets exhibit poor stable attachment to fibrinogen, reduced surface contact areas in spreading platelets, and loss of actin-rich structures under flow. (4) ADAP transduces outside-in αIIbβ3 signals to organize the localization of proteins, including vinculin and VASP, and under shear stress by enabling signal relay from Src family kinases to the platelet actin cytoskeleton to appropriately localize SLP-76 and to promote Vav1 tyrosine phosphorylation and lamellipodia formation.

Thus, the required role for ADAP in flow-dependent platelet adhesion and spreading onto fibrinogen, and possibly other αIIbβ3 ligands, suggests that ADAP enhances the stability of thrombi formed in the arterial circulation. The selective abnormality in thrombus formation in ADAP$^{-/-}$ mice at lower ferric chloride concentrations may furthermore reflect differences in the relative role of ADAP in tissue factor/fibrin versus collagen driven pathways.[46,47] The presence of abundant actin-rich structures under shear stress conditions in ADAP$^{+/+}$ platelets correlated with stable adhesion and thrombus formation. Similar structures were recently reported by Calaminus et al, and were hypothesized to be an early stage in platelet spreading.[48] Interestingly, under shear stress these structures persist even when platelets are well spread but largely lacking actin stress fibers, and they colocalize with active Src pTyr-418 (Figure 5). Thus, these actin-rich structures may help to promote stable anchorage of platelets to the substratum under shear stress.

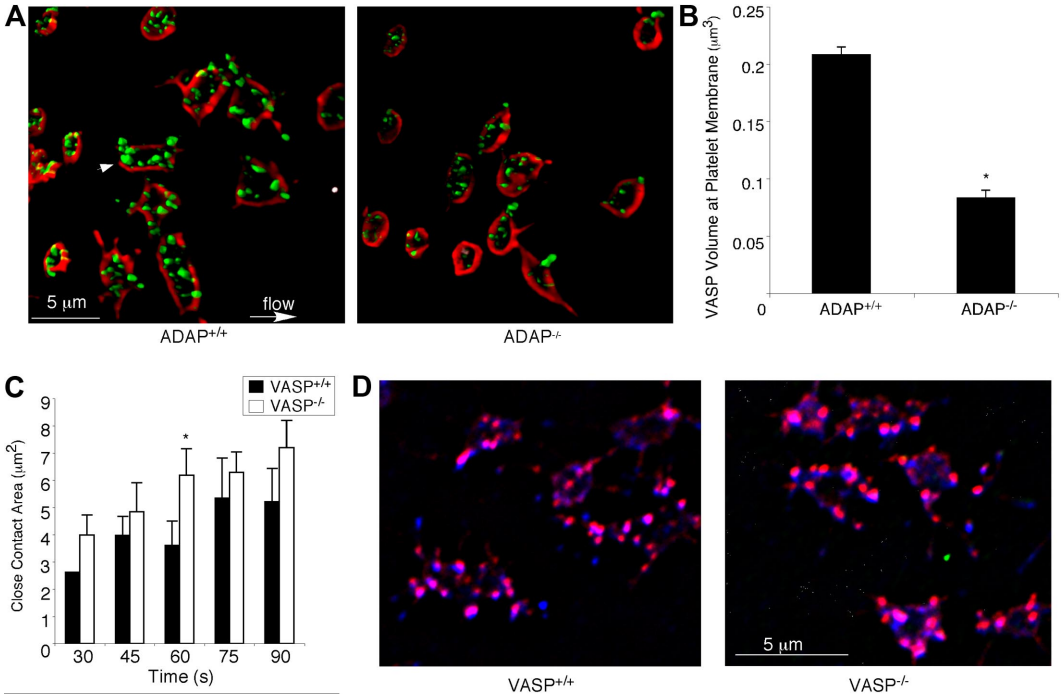

Figure 7. ADAP regulates VASP localization during outside-in αIIbβ3 signaling under shear flow. (A) Perfusion-fixed ADAP$^{+/+}$ (left) and ADAP$^{-/-}$ (right) platelets captured onto fibrinogen were stained for VASP (green) and GP IX (red) to delineate membranes. Three-dimensional reconstructions were made from acquired stacks of 0.1-μm image slices by the use of Volocity software. Note VASP clusters near the membrane (arrowhead). (B) Quantification of VASP fluorescence at the membrane, determined from 3-dimensional images prepared as in panel A. Platelets were costained with antibodies against VASP and GPIX, and the average overlapping volume fluorescence was calculated per platelet. Results shown are the average of 3 experiments ± SEM. *$P < .05$. (C-D) Spreading on fibrinogen under shear flow was examined in platelets from VASP-deficient mice and their littermate controls. The average close surface contact area per platelet over the course of 1.5 minutes, quantified from RICM images acquired in real time (see "Image analysis" and the legend to Figure 2 for details), is shown in panel C. *Statistically significant increase in the area of VASP$^{-/-}$ platelets relative to controls at this time point. (D) The colocalization of actin (red) and ADAP (blue) is shown. Note that actin-rich structures to which ADAP also localizes are present in both VASP$^{+/+}$ (left) and VASP$^{-/-}$ (right) platelets. Results are representative of at least 3 separate experiments.

Signaling pathways triggered by shear stress provide cues for differentiation of stem cells,[49] and they induce changes in cell morphology, stiffness, and gene expression in endothelial cells,[3,50] where stress-induced signals are superposed on ongoing signaling sustained through cell-matrix adhesions. In platelets, signaling to, and force transmission by, the cytoskeleton under the stringent time and force constraints of shear flow is expected to be an important mechanism for stable adhesion and spreading. In theory, shear stresses may trigger αIIbβ3 signaling pathways by direct structural modification of αIIbβ3, by membrane fluidity changes affecting αIIbβ3 clustering, or by altering associations of regulatory proteins with the cytoplasmic tails of αIIb and β3.[8] How might ADAP function as a mechanotransducer of αIIbβ3 signals under these conditions? Because no direct actin regulation by ADAP is known, mechanical forces transmitted to ADAP may modulate the actin-regulatory function of one or more of its binding partners, including SLP-76, Fyn, VASP, and SKAP-HOM. For example, ADAP may itself undergo shear-dependent phosphorylation and increase in binding affinity for its partners. Alternatively, shear forces on ADAP might enhance intracellular transport of associated binding partners along microtubule networks by its association with dynein, a microtubule motor protein,[51,52] or enhance membrane retention of the ADAP signaling module via ADAP's phospholipid binding domains.[15]

Of the several binding partners for ADAP, only SLP-76 has been shown to have an unambiguous role in outside-in αIIbβ3 signaling. SLP-76 expression drives lamellipodia formation,[17] and SLP-76–deficient platelets have a spreading defect, even under static conditions.[39] Mice have been generated with phenylalanine substitutions of 1 or more of 3 SLP-76 tyrosine residues that when phosphorylated recruit actin-regulatory proteins such as Vav1 and the Itk/Btk/Tec protein tyrosine kinases.[40,53,54] In particular, the loss of 2 phosphotyrosines in SLP-76 that anchor Vav1 (pTyr-112; pTyr-128) resulted in reduced platelet spreading on fibrinogen under static conditions, indicative of a key role for the SLP-76/Vav1 module in outside-in αIIbβ3 signaling.[40] Indeed, major findings in the present study were a loss of SLP-76 and Vav1 localization to actin structures and a failure of Vav1 to become phosphorylated on Tyr-174 upon adhesion of ADAP$^{-/-}$ platelets to fibrinogen under fluid shear stress (Figure 5).

These results further highlight key roles for SLP-76 and Vav1, and they establish ADAP as a critical member of this signaling module for cytoskeletal regulation and the stability of platelet adhesion to fibrinogen under shear. The involvement of Vav1 in these events presumably reflects its Rac1 exchange function and the induction of lamellipodia by Rac1.[34] Although Vav1 additionally has GEF activity toward Cdc42, filopodia formation appears to be unaffected in ADAP$^{-/-}$ platelets under flow. This finding suggests that in ADAP$^{-/-}$ platelets under flow, alternate pathways may be operating that lead to activation of Cdc42 or formins, both of which have been shown to regulate filopodia formation.[55] In addition to promoting lamellipodia formation,[56] phospho-Vav1 has been shown to regulate the stability of clusters containing Vav1 and other proteins in T cells[57] and to regulate decoupling of cortical actin from the membrane leading to increased cell deformation with applied force.[58] Because the spherical morphology of fibrinogen-adherent ADAP$^{-/-}$ platelets appears to represent an early stage of platelet spreading under flow,[59] we speculate that mislocalization of SLP-76 and loss of Vav1 functions may contribute, at least in part, to the ADAP$^{-/-}$ platelet phenotype we

observed. Interestingly, we found no gross morphologic abnormalities in platelets under flow in platelets deficient in either one of ADAP's 2 other binding partners, SKAP-HOM or VASP.

In conclusion, this study provides a new understanding of the responses of platelets to mechanotransduction initiated through αIIbβ3 under hydrodynamic stress conditions by establishing an essential role for ADAP in this process. Further studies will be required to determine precisely how mechanical forces engendered by hemodynamic shear stresses affect ADAP's function downstream of αIIbβ3 to transmit adhesive signals to the platelet cytoskeleton.

Acknowledgments

We are grateful to Alexander Clowes for providing VASP-deficient mice, Gary Koretzky for providing ADAP-deficient mice, and Ben Neel for the SKAP-HOM–deficient mice. We thank Meri Ripani for technical assistance with image analysis and Per Fogelstrand for providing expertise on surgical procedures in the mouse.

This work was supported by grants HL78784, HL31950, and HL56595 from the National Institutes of Health

Authorship

Contribution: A.K.-F. performed the experiments and analyzed the data; Z.M.R. supplied vital reagents; and A.K.-F., Z.M.R., and S.J.S. designed the research and wrote the paper.

Conflict-of-interest disclosure: The authors declare no competing financial interests.

Correspondence: Dr Ana Kasirer-Friede, Department of Medicine, University of California, San Diego, 9500 Gilman Dr, Mail Code 0726, La Jolla, CA 92093-0726; e-mail: akasirer@ucsd.edu/sshattil@ucsd.edu.

References

1. Ruggeri ZM. Platelet adhesion under flow. *Microcirculation.* 2009;16(1):58-83.
2. Shattil SJ, Newman PJ. Integrins: dynamic scaffolds for adhesion and signaling in platelets. *Blood.* 2004;104(6):1606-1615.
3. Davies PF. Flow-mediated endothelial mechanotransduction. *Physiol Rev.* 1995;75(3):519-560.
4. Helmke BP, Thakker DB, Goldman RD, Davies PF. Spatiotemporal analysis of flow-induced intermediate filament displacement in living endothelial cells. *Biophys J.* 2001;80(1):184-194.
5. Hahn C, Schwartz MA. Mechanotransduction in vascular physiology and atherogenesis. *Nat Rev Mol Cell Biol.* 2009;10(1):53-62.
6. Yap CL, Anderson KE, Hughan SC, Dopheide SM, Salem HH, Jackson SP. Essential role for phosphoinositide 3-kinase in shear-dependent signaling between platelet glycoprotein Ib/V/IX and integrin alpha(IIb)beta(3). *Blood.* 2002;99(1):151-158.
7. Mazzucato M, Cozzi MR, Pradella P, Ruggeri ZM, De Marco L. Distinct roles of ADP receptors in von Willebrand factor-mediated platelet signaling and activation under high flow. *Blood.* 2004;104(10):3221-3227.
8. Feng S, Lu X, Resendiz JC, Kroll MH. Pathological shear stress directly regulates platelet alphaIIbbeta3 signaling. *Am J Physiol Cell Physiol.* 2006;291(6):C1346-C1354.
9. Peterson EJ. The TCR ADAPts to integrin-mediated cell adhesion. *Immunol Rev.* 2003;192:113-121.
10. Wang H, Rudd CE. SKAP-55, SKAP-55–related and ADAP adaptors modulate integrin-mediated immune-cell adhesion. *Trends Cell Biol.* 2008;18(10):486-493.
11. Marie-Cardine A, Hendricks-Taylor LR, Boerth NJ, Zhao H, Schraven B, Koretzky GA. Molecular interaction between the Fyn-associated protein SKAP55 and the SLP-76-associated phosphoprotein SLAP-130. *J Biol Chem.* 1998;273(40):25789-25795.
12. Marie-Cardine A, Verhagen AM, Eckerskorn C, Schraven B. SKAP-HOM, a novel adaptor protein homologous to the FYN-associated protein SKAP55. *FEBS Lett.* 1998;435(1):55-60.
13. Ménasche G, Kliche S, Chen EJ, Stradal TE, Schraven B, Koretzky G. RIAM links the ADAP/SKAP-55 signaling module to Rap1, facilitating T-cell receptor–mediated integrin activation. *Mol Cell Biol.* 2007;27(11):4070-4081.
14. Medeiros RB, Burbach BJ, Mueller KL, et al. Regulation of NF-kappaB activation in T cells via association of the adapter proteins ADAP and CARMA1. *Science.* 2007;316(5825):754-758.
15. Heuer K, Arbuzova A, Strauss H, Kofler M, Freund C. The helically extended SH3 domain of the T-cell adaptor protein ADAP is a novel lipid interaction domain. *J Mol Biol.* 2005;348(4):1025-1035.
16. Kasirer-Friede A, Moran B, Nagrampa-Orje J, et al. ADAP is required for normal alphaIIbbeta3 activation by VWF/GP Ib-IX-V and other agonists. *Blood.* 2007;109(3):1018-1025.
17. Obergfell A, Judd BA, del Pozo MA, Schwartz MA, Koretzky GA, Shattil SJ. The molecular adapter SLP-76 relays signals from platelet integrin alphaIIbbeta3 to the actin cytoskeleton. *J Biol Chem.* 2001;276(8):5916-5923.
18. Peterson EJ, Woods ML, Dmowski SA, et al. Coupling of the TCR to integrin activation by Slap-130/Fyb. *Science.* 2001;293(5538):2263-2265.
19. Togni M, Swanson KD, Reimann S, et al. Regulation of in vitro and in vivo immune functions by the cytosolic adaptor protein SKAP-HOM. *Mol Cell Biol.* 2005;25(18):8052-8063.
20. Hauser W, Knobeloch KP, Eigenthaler M, et al. Megakaryocyte hyperplasia and enhanced agonist-induced platelet activation in vasodilator-stimulated phosphoprotein knockout mice. *Proc Natl Acad Sci U S A.* 1999;96(14):8120-8125.
21. Massberg S, Gruner S, Konrad I, et al. Enhanced in vivo platelet adhesion in vasodilator-stimulated phosphoprotein (VASP)-deficient mice. *Blood.* 2004;103(1):136-142.
22. Ablooglu AJ, Kang J, Petrich BG, Ginsberg MH, Shattil SJ. Antithrombotic effects of targeting alphaIIbbeta3 signaling in platelets. *Blood.* 2009;113(15):3585-3592.
23. Savage B, Saldivar E, Ruggeri ZM. Initiation of platelet adhesion by arrest onto fibrinogen or translocation on von Willebrand factor. *Cell.* 1996;84(2):289-297.
24. Curtis AS. The mechanism of adhesion of cells to glass: a study by interference reflection microscopy. *J Cell Biol.* 1964;20:199-215.
25. Kloboucek A, Behrisch A, Faix J, Sackmann E. Adhesion-induced receptor segregation and adhesion plaque formation: a model membrane study. *Biophys J.* 1999;77(4):2311-2328.
26. Reininger AJ, Heijnen HF, Schumann H, Specht HM, Schramm W, Ruggeri ZM. Mechanism of platelet adhesion to von Willebrand factor and microparticle formation under high shear stress. *Blood.* 2006;107(9):3537-3545.
27. Kato K, Kanaji T, Russell S, et al. The contribution of glycoprotein VI to stable platelet adhesion and thrombus formation illustrated by targeted gene deletion. *Blood.* 2003;102(5):1701-1707.
28. Soriani A, Moran B, de Virgilio M, et al. A role for PKCtheta in outside-in alpha(IIb)beta3 signaling. *J Thromb Haemost.* 2006;4(3):648-655.
29. Chow S, Hedley D, Grom P, Magari R, Jacobberger JW, Shankey TV. Whole blood fixation and permeabilization protocol with red blood cell lysis for flow cytometry of intracellular phosphorylated epitopes in leukocyte subpopulations. *Cytometry A.* 2005;67(1):4-17.
30. Kasirer-Friede A, Cozzi MR, Mazzucato M, De Marco L, Ruggeri ZM, Shattil SJ. Signaling through GP Ib-IX-V activates alpha IIb beta 3 independently of other receptors. *Blood.* 2004;103(9):3403-3411.
31. Arias-Salgado EG, Haj F, Dubois C, et al. PTP-1B is an essential positive regulator of platelet integrin signaling. *J Cell Biol.* 2005;170(5):837-845.
32. Andre P, Delaney SM, LaRocca T, et al. P2Y12 regulates platelet adhesion/activation, thrombus growth, and thrombus stability in injured arteries. *J Clin Invest.* 2003;112(3):398-406.
33. Goschnick MW, Lau LM, Wee JL, et al. Impaired "outside-in" integrin alphaIIbbeta3 signaling and thrombus stability in TSSC6-deficient mice. *Blood.* 2006;108(6):1911-1918.
34. McCarty OJ, Larson MK, Auger JM, et al. Rac1 is essential for platelet lamellipodia formation and aggregate stability under flow. *J Biol Chem.* 2005;280(47):39474-39484.
35. Wu YP, de Groot PG, Sixma JJ. Shear-stress-induced detachment of blood platelets from various surfaces. *Arterioscler Thromb Vasc Biol.* 1997;17(11):3202-3207.
36. Nachmias VT, Golla R. Vinculin in relation to stress fibers in spread platelets. *Cell Motil Cytoskeleton.* 1991;20(3):190-202.
37. Yin H, Liu J, Li Z, Berndt MC, Lowell CA, Du X. Src family tyrosine kinase Lyn mediates VWF/GPIb-IX-induced platelet activation via the cGMP signaling pathway. *Blood.* 2008;112(4):1139-1146.
38. Wang H, Wei B, Bismuth G, Rudd CE. SLP-76-ADAP adaptor module regulates LFA-1 mediated costimulation and T-cell motility. *Proc Natl Acad Sci U S A.* 2009;106(30):12436-12441.
39. Judd BA, Myung PS, Leng L, et al. Hematopoietic reconstitution of SLP-76 corrects hemostasis and platelet signaling through alpha IIb beta 3 and collagen receptors. *Proc Natl Acad Sci U S A.* 2000;97(22):12056-12061.

40. Bezman NA, Lian L, Abrams CS, et al. Requirements of SLP76 tyrosines in ITAM and integrin receptor signaling and in platelet function in vivo. *J Exp Med.* 2008;205(8):1775-1788.

41. Breitsprecher D, Kiesewetter AK, Linkner J, et al. Clustering of VASP actively drives processive, WH2 domain-mediated actin filament elongation. *EMBO J.* 2008;27(22):2943-2954.

42. Schirenbeck A, Arasada R, Bretschneider T, Stradal TE, Schleicher M, Faix J. The bundling activity of vasodilator-stimulated phosphoprotein is required for filopodium formation. *Proc Natl Acad Sci U S A.* 2006;103(20):7694-7699.

43. Swanson KD, Tang Y, Ceccarelli DF, et al. The Skap-hom dimerization and PH domains comprise a 3′-phosphoinositide-gated molecular switch. *Mol Cell.* 2008;32(4):564-575.

44. Aghazadeh B, Lowry WE, Huang XY, Rosen MK. Structural basis for relief of autoinhibition of the Dbl homology domain of proto-oncogene Vav by tyrosine phosphorylation. *Cell.* 2000;102(5):625-633.

45. Rottner K, Behrendt B, Small JV, Wehland J. VASP dynamics during lamellipodia protrusion. *Nat Cell Biol.* 1999;1(5):321-322.

46. Wang X, Cheng Q, Xu L, et al. Effects of factor IX or factor XI deficiency on ferric chloride-induced carotid artery occlusion in mice. *J Thromb Haemost.* 2005;3(4):695-702.

47. Dubois C, Panicot-Dubois L, Merrill-Skoloff G, Furie B, Furie BC. Glycoprotein VI-dependent and -independent pathways of thrombus formation in vivo. *Blood.* 2006;107(10):3902-3906.

48. Calaminus SD, Thomas S, McCarty OJ, Machesky LM, Watson SP. Identification of a novel, actin-rich structure, the actin nodule, in the early stages of platelet spreading. *J Thromb Haemost.* 2008;6(11):1944-1952.

49. Adamo L, Naveiras O, Wenzel PL, et al. Biomechanical forces promote embryonic haematopoiesis. *Nature.* 2009;459(7250):1131-1135.

50. del Alamo JC, Norwich GN, Li YS, Lasheras JC, Chien S. Anisotropic rheology and directional mechanotransduction in vascular endothelial cells. *Proc Natl Acad Sci U S A.* 2008;105(40):15411-15416.

51. Combs J, Kim SJ, Tan S, et al. Recruitment of dynein to the Jurkat immunological synapse. *Proc Natl Acad Sci U S A.* 2006;103(40):14883-14888.

52. Rothwell SW, Calvert VS. Activation of human platelets causes post-translational modifications to cytoplasmic dynein. *Thromb Haemost.* 1997;78(2):910-918.

53. Jordan MS, Sadler J, Austin JE, et al. Functional hierarchy of the N-terminal tyrosines of SLP-76. *J Immunol.* 2006;176(4):2430-2438.

54. Reeve JL, Zou W, Liu Y, Maltzman JS, Ross FP, Teitelbaum SL. SLP-76 couples Syk to the osteoclast cytoskeleton. *J Immunol.* 2009;183:1804-1812.

55. Faix J, Breitsprecher D, Stradal TE, Rottner K. Filopodia: complex models for simple rods. *Int J Biochem Cell Biol.* 2009;41(8-9):1656-1664.

56. Crespo P, Schuebel KE, Ostrom AA, Gutkind JS, Bustelo XR. Phosphotyrosine-dependent activation of Rac-1 GDP/GTP exchange by the vav proto-oncogene product. *Nature.* 1997;385(6612):169-172.

57. Miletic AV, Sakata-Sogawa K, Hiroshima M, et al. Vav1 acidic region tyrosine 174 is required for the formation of T-cell receptor-induced microclusters and is essential in T-cell development and activation. *J Biol Chem.* 2006;281(50):38257-38265.

58. Faure S, Salazar-Fontana LI, Semichon M, et al. ERM proteins regulate cytoskeleton relaxation promoting T-cell–APC conjugation. *Nat Immunol.* 2004;5(3):272-279.

59. Maxwell MJ, Dopheide SM, Turner SJ, Jackson SP. Shear induces a unique series of morphological changes in translocating platelets: effects of morphology on translocation dynamics. *Arterioscler Thromb Vasc Biol.* 2006;26(3):663-669.